ORIGINAL PAPER

Morphology and internal structure of copper deposits electrodeposited by the pulsating current regime in the hydrogen co-deposition range

Nebojša D. Nikolić · Goran Branković · Vesna M. Maksimović

Abstract The effect of the regime of pulsating current (PC) on copper electrodeposition in the hydrogen co-deposition range was examined by the techniques of scanning electron and optical microscopes. The quantities of evolved hydrogen and morphologies of electrodeposited copper strongly depended on the applied parameters of square waves PC, such as the current density amplitude (or the amplitude of the cathodic current density), deposition pulse, and pause duration. The increase of the current density amplitude led to intensification of hydrogen evolution reaction, and the change of morphology of electrodeposited copper from dendrites and shallow holes to dish-like holes was observed. For the constant pause duration, the prolonging deposition pulses intensify hydrogen evolution reaction leading to the formation of the honeycomb-like structures. The set of modified equations considering the effect of hydrogen generated during metal electrodeposition processes by the pulsating current regime is also presented. The concept of "effective overpotential amplitude" was proposed to explain the change of copper surface morphology with the intensification of hydrogen evolution reaction.

N. D. Nikolić (✉)
ICTM—Institute of Electrochemistry, University of Belgrade,
Njegoševa 12,
Belgrade, Serbia
e-mail: nnikolic@tmf.bg.ac.rs

G. Branković
Institute for Multidisciplinary Research, University of Belgrade,
Belgrade, Serbia

V. M. Maksimović
Department of material science, INN Vinča,
University of Belgrade,
Belgrade, Serbia

Introduction

The 3D foam or honeycomb-like structure is the type of irregular metal deposits which is of high both academic and technological significance. In constant regimes of electrolysis, this type of deposits is formed by electrodeposition processes at high overpotentials or current densities where parallel to metal electrodeposition, hydrogen evolution reaction occurs. The main characteristics of this deposit type are micro-sized holes or pores formed due to attached hydrogen bubbles and cauliflower-like agglomerates of metal grains or dendrites formed around them [1–3]. The number, size, and distribution of holes in 3D foam or the honeycomb-like structures can be easily controlled by the choice of appropriate electrolysis parameters [4–6]. Also, the size of grains constructing dendrites or cauliflower-like agglomerates formed around holes, as well as the size of channels between small metal grains agglomerates are controlled by conditions of electrolysis. Due to open porous structure with the extremely high surface area, 3D foam or the honeycomb-like structures are very suitable to be used as electrodes in many electrochemical devices, such as fuel cells, batteries, and sensors [2, 7, 8], as well as in catalytic purpose [9]. For example, this type of structure is together with some thin film technologies of special importance in the development of electrodes for Li-ion batteries [8, 10, 11]. Formation of copper structures with such characteristics is the most detailed studied system [1–6, 8, 12, 13], although formation of these structures of some other metals, such as tin [2], nickel [14], and silver [15, 16], was also investigated.

For structural analysis of open porous structures with the extremely high surface area (the honeycomb-like structures), the techniques of scanning electron (SEM) and optical microscopes are widely used [3, 17]. The SEM technique gives information concerning surface morphology ("top view") of deposits. For the purpose of the analysis of internal structure (cross-section analysis) of these deposits, the use of optical microscope is preferable [17].

In the last time, the improvement of micro- and nano-structural characteristics of the honeycomb-like structures related to those obtained in the constant regimes of electrolysis was attained by the application of periodically changing regimes of electrolysis, such as pulsating over-potential (PO) [18–20] and pulsating current (PC) regimes [21]. Effects attained by the application of these regimes of electrolysis on micro- and nanostructural characteristics of copper deposits were equivalent to those attained by the addition of additives in electroplating solutions [4, 22, 23].

The regime of PO is primarily important from academic point of view for understanding of mechanism of electro-deposition processes at periodically changing rate. For technological purposes, pulse and reverse plating techniques, such as PC and reversing current (RC), are more important [24, 25]. Considering the possibility of the application of the PC regime on the formation of copper electrodes of the high technological significance, the detailed analysis of the effect of different parameters of this regime of electrolysis on copper electrodeposition processes in the hydrogen co-deposition range is needed. For that reason, the aim of this paper is a continuation of investigation of the effect of the PC regime on copper electrodeposition in the hydrogen co-deposition range.

Experimental

Copper was electrodeposited from 0.15 M CuSO$_4$ in 0.50 M H$_2$SO$_4$, in an open cell at the room temperature. Doubly distilled water and analytical grade chemicals were used for the preparation of the solution for electrodeposition of copper. Copper electrodeposition was performed by the use of the regime of PC. The following parameters of square waves PC were analyzed:

(a) The current density amplitude 0.20 A/cm^2, deposition pulses 1 and 2 ms, pause duration 10 ms
(b) The current density amplitude 0.44 A/cm^2; deposition pulses 1, 4, 7, 10, and 20 ms; pause duration 10 ms

The working electrodes used for electrodeposition of copper were cylindrical copper wires. The surface area of the working electrodes, S_0, was 0.25 cm^2. The counter electrode was copper foil of 0.80 dm^2 surface area placed close to the walls of the cell. The working electrode was situated in the center of cell at the same location for each experiment. The distance between the working and the counter electrode was 23 mm.

The preparation of working electrodes consisted of alkaline degreasing at 70 °C followed by an acid etching (20% H$_2$SO$_4$) at 50 °C. After each phase, working electrodes were rinsed with distilled water. This pretreatment of the electrodes was important in order to obtain the same initial electrode surface prior to the each experiment.

Copper was electrodeposited with quantities of electricity of 10 mA h/cm^2. The obtained copper deposits were characterized using a scanning electron microscope—TESCAN Digital Microscopy.

Cross-section analysis of the copper electrodes was performed using Zeiss Axiovert 25 optical microscope equipped with digital camera Panasonic WV-CD50. In order to observe the cross section of obtained deposit, the electrode together with the deposit was mounted and fixed by the epoxy resin. In that way, the cross section was represented the plain parallel to the line of deposit growth. Samples were polished several times and cross-section structure was observed in non-etching state.

The average current efficiency of hydrogen evolution, $\eta_{I,av}(H_2)$, was already determined by the use of experimental procedure described in [21, 26].

Results and discussion

The regime of PC consists of a periodic repetition of square pulses [24], and it is characterized by the amplitude of the cathodic current density, j_A; the deposition pulse, t_c (on period); and the pause duration, t_p, in which the system relaxes (off period). The average current density, j_{av}, is given by Eq. 1:

$$j_{av} = \frac{j_A t_c}{t_c + t_p} \tag{1}$$

or

$$j_{av} = \frac{j_A}{1 + p} \tag{2}$$

if

$$p = \frac{t_p}{t_c} \tag{3}$$

where p is the pause-to-pulse ratio.

In the PC regimes, the surface concentration of depositing ions is only determined by the average current density [24].

Then, the overpotential amplitude, η_A, can be presented by Eq. 4 [27]:

$$\eta_A = \frac{b_c}{2.3} \ln \frac{j_{av}(p+1)}{j_0} + \frac{b_c}{2.3} \ln \frac{1}{1 - \frac{j_{av}}{j_L}} \quad (4)$$

where b_c is the cathodic Tafel slope, j_L is the limiting diffusion current density, and j_0 is the exchange current density. The activation part of overpotential, η_{act} is

$$\eta_{act} = \frac{b_c}{2.3} \ln \frac{j_{av}}{j_0} (p+1) \quad (5)$$

while the diffusion part of overpotential, η_{diff} is

$$\eta_{diff} = \frac{b_c}{2.3} \ln \frac{1}{1 - \frac{j_{av}}{j_L}} \quad (6)$$

Equation 4 can be rewritten in the form:

$$\eta_A = \eta_{const} + \frac{b_c}{2.3} \ln(p+1) \quad (7)$$

where η_{const} is the overpotential in the constant regime of electrolysis defined by Eq. 8:

$$\eta_{const} = \frac{b_c}{2.3} \ln \frac{j_{av}}{j_0} + \frac{b_c}{2.3} \ln \frac{1}{1 - \frac{j_{av}}{j_L}} \quad (8)$$

if $j_{av} = j$, where j is the current density in the constant regime of electrolysis.

Equation 4 is valid in the frequency range 10–100 Hz, where the frequency is sufficiently high to produce constant concentration on the surface and sufficiently low that the effect of DC capacity can be neglected. Hence, in the analyzed frequency range from 10 to 100 Hz, the surface concentration of depositing ions is constant and equal to the one in the constant regime at the current density corresponding to the average current density in the PC regime [24, 28]. From point of view of the average current density, it means that there is no any difference between electrochemical deposition processes in the constant regimes and PC conditions. On the other hand, it is very clear from Eq. 4 that at the fixed value of the average current density, the amplitude of overpotential depends on pause-to-pulse ratio, and it increases with the increasing pause-to-pulse ratio.

According to Popov and Pavlović [27], the degree of diffusion control of electrodeposition process, ω, is defined by Eq. 9:

$$\omega = \frac{\ln \frac{1}{1 - \frac{j_{av}}{j_L}}}{\ln \frac{j_{av}}{j_0} + \ln(p+1) + \ln \frac{1}{1 - \frac{j_{av}}{j_L}}} \quad (9)$$

and it represents a contribution of diffusion overpotential to total cathode overpotential. Hence, due to the increase of activation part of overpotential with the increasing pause-

to-pulse ratio, the degree of diffusion control will decrease with the increasing pause-to-pulse ratio, resulting in the possible change of texture of deposit. It is noteworthy that it is valid if $j_{av} < j_L$ in the mixed controlled deposition.

In the hydrogen co-deposition range, the current efficiency for metal electrodeposition is less than 1, and then, similar to the RC regime [29], the effective average current density, j_{av}^*, can be given by Eq. 10:

$$j_{av}^* = \frac{\eta_{I,av}(M) j_A}{1 + p} \quad (10)$$

where $\eta_{I,av}(M)$ is the average current efficiency for metal electrodeposition.

Since

$$\eta_{I,av}(M) + \eta_{I,av}(H_2) = 1 \quad (11)$$

where $\eta_{I,av}(H_2)$ is the average current efficiency of hydrogen evolution, Eq. 10 can be rewritten as

$$j_{av}^* = \frac{[1 - \eta_{I,av}(H_2)] j_A}{1 + p} \quad (12)$$

and according to Eqs. 2 and 10

$$\eta_{I,av}(H_2) = 1 - \frac{j_{av}^*}{j_{av}} \quad (13)$$

In the hydrogen co-deposition range, if $j_{av} > j_L$, the amplitude of overpotential is related to the hydrogen reduction, increasing with the current density of hydrogen evolution [27]. Equation 4 is still valid [27], but it must be modified and adjusted to the effect of hydrogen evolution what will be considered in detail in this paper.

The quantities of evolved hydrogen and hence morphologies of electrodeposited metal strongly depend on the applied parameters of PC regimes, such as the amplitude of the current density, deposition pulse, and pause duration. Figure 1 shows SEM micrographs of the copper deposit obtained with the current density amplitude of 0.20 A/cm², a deposition pulse of 1 ms, and a pause of 10 ms. Very branchy dendrites (Fig. 1a, b), small cauliflower-like forms (Fig. 1a, c), and shallow holes formed from detached hydrogen bubbles (Fig. 1a, c) were obtained with these parameters of the PC regime. Formation of these morphological forms was accompanied by the quantity of evolved hydrogen which corresponded to the average current efficiency of hydrogen evolution of 5.5% [26].

In PC regimes, intensification of hydrogen evolution reaction can be achieved by:

1. The increase of the current density amplitude and keeping both the durations of the deposition pulse and pause constant

Fig. 1 The copper deposit obtained by the regime of pulsating current: **a** top view, **b** dendrite, and **c** holes formed by attached hydrogen bubbles. The current density amplitude 0.20 A/cm^2, deposition pulse 1 ms, and pause duration 10 ms
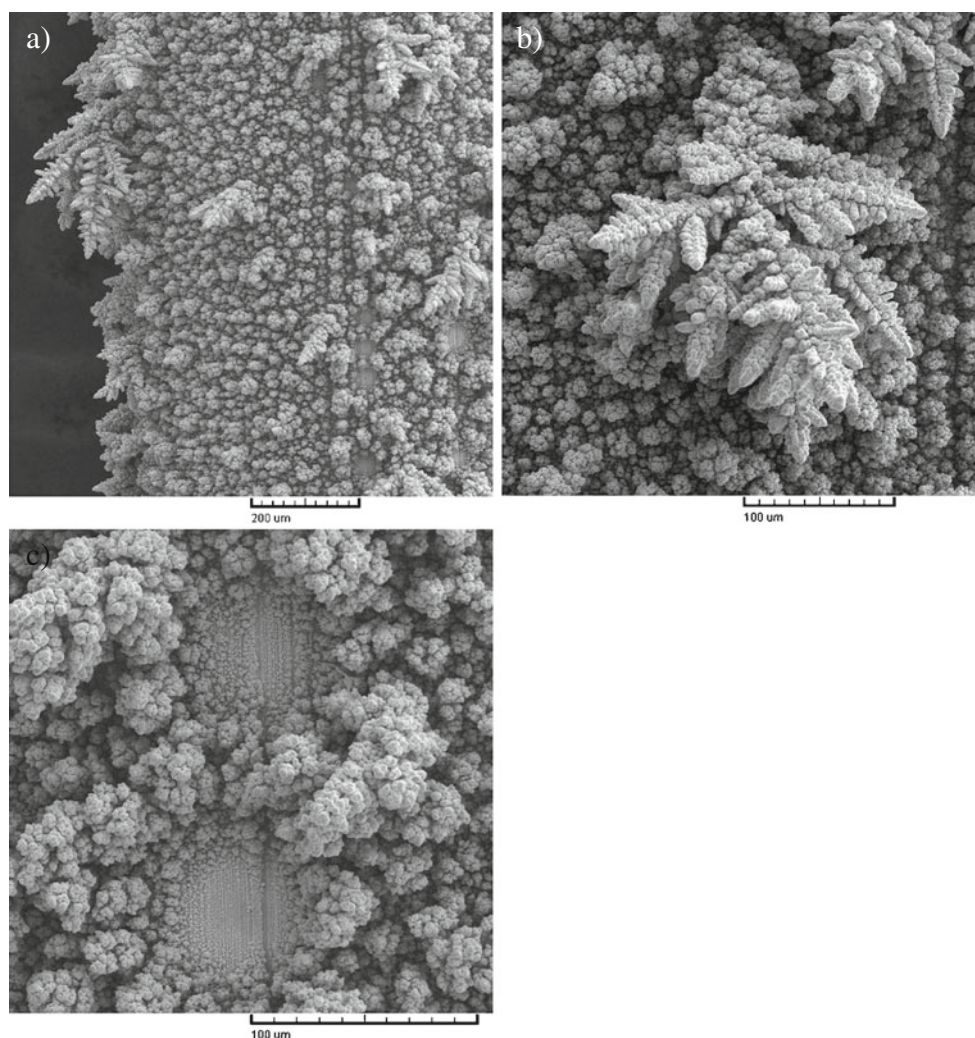
2. The prolonging of a deposition pulse duration and keeping both the current density amplitude and a pause duration constant

3. The shortening of a pause duration and keeping both the current density amplitude and a deposition pulse constant

Since the second and third ways are closely related, these two ways will be analyzed simultaneously.

Figure 2 shows SEM micrographs of copper deposits obtained with $j_A=0.44$ A/cm^2, $t_c=1$ ms, and $t_p=10$ ms (Fig. 2a), as well as with $j_A=0.20$ A/cm^2, $t_c=2$ ms, and $t_p=10$ ms (Fig. 2b). The quantities of hydrogen generated during copper electrodeposition processes by these parameters of square waves PC corresponded to the average current efficiencies of hydrogen evolution, $\eta_{I,av}(H_2)$, of 13.7% for the square wave PC composed of $j_A=0.44$ A/cm^2, $t_c=1$ ms, and $t_p=10$ ms [21] and 10.3% for the square wave PC composed of $j_A=0.20$ A/cm^2, $t_c=2$ ms, and $t_p=10$ ms [26].

From Fig. 2a, it can be seen that intensification of hydrogen evolution caused by the increase of the current density amplitude (the first way) led to the formation of dish-like holes. Aside from dish-like holes, small independently formed cauliflower-like agglomerates of copper grains were obtained with these parameters of the PC regime.

Keeping both the current density amplitude and pause duration constant (the second way), intensification of hydrogen evolution reaction caused by the prolongation of a deposition pulse led to the increase of number of holes which the origin was of evolved hydrogen, as well as to the appearing of dish-like holes (Fig. 2b). Also, the mixture of degenerate dendrites and cauliflower-like agglomerates of copper grains was formed with a deposition pulse of 2 ms (Fig. 2b).

The further intensification of hydrogen evolution reaction with the prolongation of the deposition pulse leads to the formation of the honeycomb-like structures with the both current density amplitude applied. Figure 3a, b shows the typical honeycomb-like structures obtained by the PC regimes with $j_A=0.20$ A/cm^2, $t_c=50$ ms, and $t_p=10$ ms (Fig. 3a), as well as with $j_A=0.44$ A/cm^2, $t_c=10$ ms, and

Fig. 2 Copper deposits obtained by the PC regimes: **a** the current density amplitude 0.44 A/cm^2, deposition pulse 1 ms, and pause duration 10 ms and **b** the current density amplitude 0.20 A/cm^2, deposition pulse 2 ms, and pause duration 10 ms
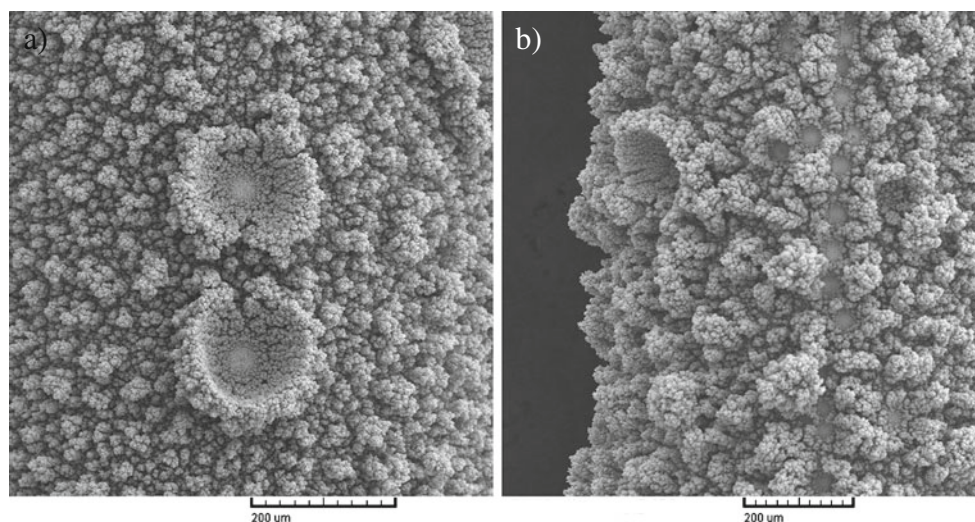
t_p=10 ms (Fig. 3b). The average current efficiencies of hydrogen evolution, $\eta_{I,av}(H_2)$, were 27.2% (for the honeycomb-like structure shown in Fig. 3a) and 30.0% (for the honeycomb-like structure shown in Fig. 3b). The

typical elements of which the honeycomb-like structure type is constructed, such as holes formed by attached hydrogen bubbles and cauliflower-like agglomerates of copper grains formed around them obtained by the PC

Fig. 3 The honeycomb-like structures obtained by the PC regimes with: **a** j_A=0.20 A/cm^2, t_c=50 ms, and t_p=10 ms; **b** j_A= 0.44 A/cm^2, t_c=10 ms, and t_p= 10 ms. The typical elements of the honeycomb-like structure obtained by the PC regime with j_A=0.44 A/cm^2, t_c=10 ms, and t_p=10 ms: **c** hole and **d** cauliflower-like agglomerates of copper grains
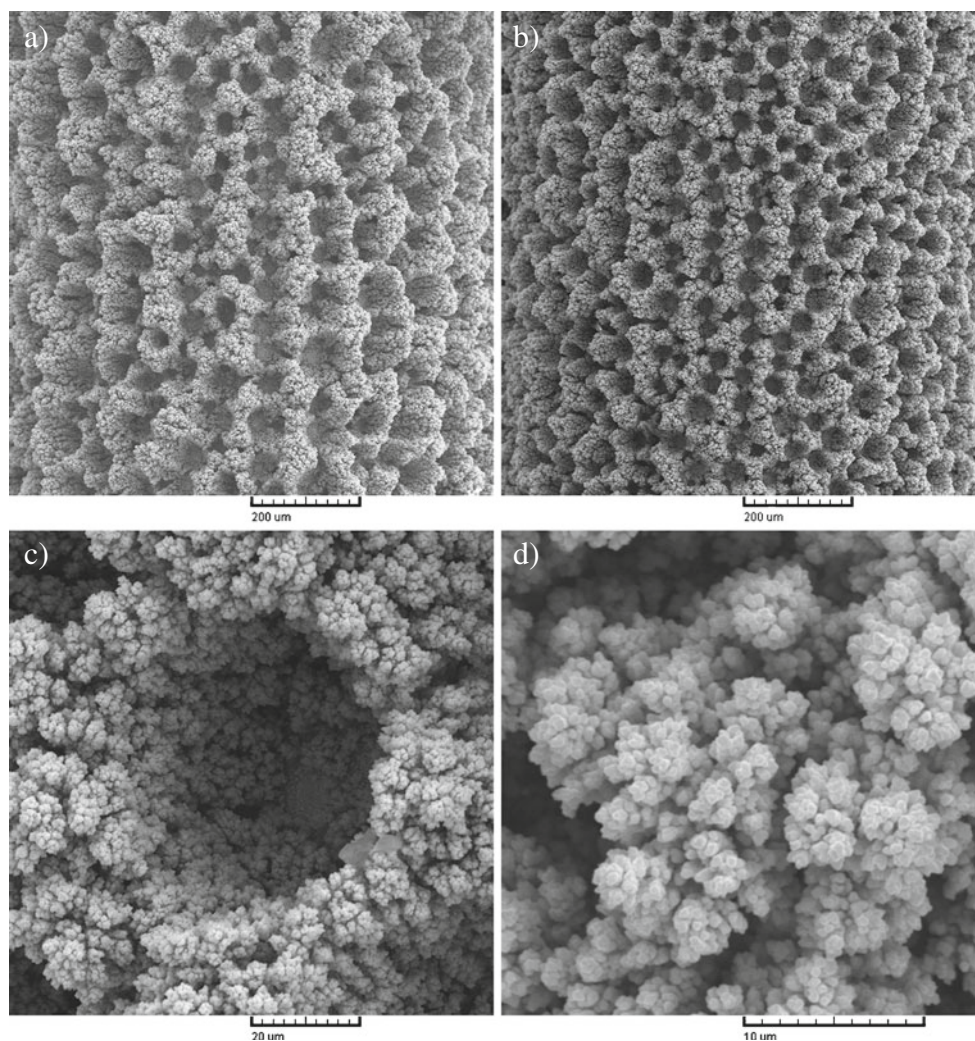
regime with j_A=0.44 A/cm^2, t_c=10 ms, and t_p=10 ms are shown in Fig. 3c, d, respectively.

Formation of the honeycomb-like structure by the PC regimes will be analyzed applying the current density amplitude of 0.44 A/cm^2, a pause duration of 10 ms, and different lengths of deposition pulses (the second way). Figure 4 shows the dependences of the effective average current density, $j_{av}*$, and the average current efficiency of hydrogen evolution, $\eta_{I,av}(H_2)$, on pause-to-pulse ratio, p. From Fig. 4, it can be seen that the increasing pause-to-pulse ratio leads to the decrease of both $j_{av}*$ and $\eta_{I,av}(H_2)$. The honeycomb-like structures are formed with a pause-to-pulse ratio smaller than 1.43 [21], i.e., with deposition pulses longer than 7 ms (for a pause duration of 10 ms). On the other hand, the mixture of dish-like holes and holes constructing the honeycomb-like structure was obtained with a pause-to-pulse ratio of 2.5 (t_c=4 ms; t_p=10 ms) [21]. Finally, as already shown in Fig. 2a, dish-like holes were only formed with a deposition pulse of 1 ms (p=10).

Figure 5 shows cross sections of copper deposits obtained with deposition pulses of 4, 7, 10, and 20 ms. From Fig. 5, it can be seen that the interior of these structures was very porous and consisted of disperse particles surrounded by irregular channels which the origin is of evolved hydrogen. Also, it is necessary to note that dispersity of particles increased, i.e., dendritic character of particles decreased with the prolonging duration of deposition pulse.

The change of morphology of electrodeposited copper from very branchy dendrites and dish-like holes to the honeycomb-like structures can be explained by the analysis of the effectiveness of solution stirring by evolved hydrogen in the following way: the effectiveness of stirring of the solution by hydrogen generated at the cathode surface during electrochemical deposition process increases with intensification of hydrogen evolution reaction. In the
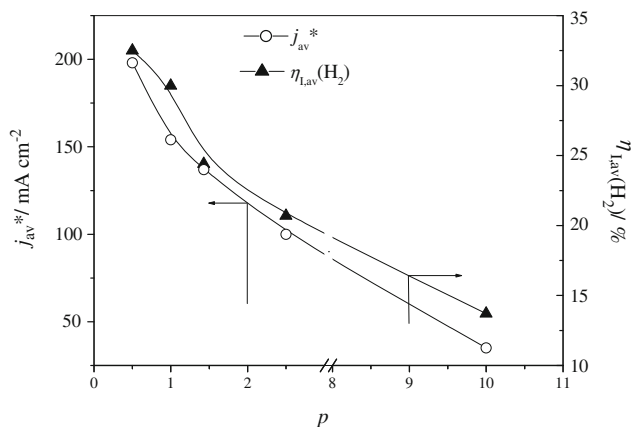
one moment, hydrogen evolution will become vigorous enough to cause the decrease of the cathode diffusion layer thickness and the increase of the limiting diffusion current density leading to the change of the hydrodynamic conditions in the near-electrode layer [3]. According to Eqs. 4 and 9, it means the decrease of the degree of diffusion control of electrodeposition process with intensification of hydrogen evolution reaction. The degree of diffusion control of electrodeposition process will additionally decrease due to the smaller values of the effective average current densities, $j_{av}*$, in relation to those obtained in the absence of hydrogen evolution (Eqs. 2 and 12). Then, the overpotential amplitude corresponding to copper electrodeposition will be smaller than the one specified by pulse rectifiers, and this value is denoted as effective overpotential amplitude. Equation 4 modified and adapted to the case of copper electrodeposition in the hydrogen co-deposition range can be presented as:

$$\eta_{A,eff} = \frac{b_c}{2.3} \ln \frac{j_{av}*(p+1)}{j_0} + \frac{b_c}{2.3} \ln \frac{1}{1 - \frac{j_{av}*}{j_L}} \qquad (14)$$

Hence, the effective overpotential amplitude, $\eta_{A,eff}$, will decrease with the intensification of hydrogen evolution reaction due to the decrease of the degree of diffusion control of electrodeposition process. So, the validity of the concept of "effective overpotential" can be expanded to include metal electrodeposition in the hydrogen co-deposition range by the regime of PC. The concept of "effective overpotential" is the only proposed mechanism considering metal electrochemical deposition processes in the hydrogen co-deposition range. This concept was originally proposed to explain the change of surface morphology during copper electrodeposition in the constant potentiostatic regime of electrolysis at high overpotentials where parallel to copper electrodeposition, the strong hydrogen evolution occurs [3]. According to this concept, when hydrogen evolution is vigorous enough, then electrodeposition process occurs at some overpotential which is effectively lower than the specified one, and this overpotential is denoted by "effective one" of deposition process. Increasing overpotential intensifies hydrogen evolution reaction causing stirring of the solution in the near-electrode layer. The different degrees of diffusion control are achieved by the change of overpotential of electrodeposition. From morphological point of view, the concept of "effective overpotential" means that morphologies of metal deposits become similar to those obtained at some overpotential where hydrogen evolution does not exist or it is very small.

Anyway, the decrease of dendritic character of particles and hence the increase of dispersity of particles in the formed honeycomb-like structures (Fig. 5), as well as the change of the surface morphology from dendrites (Fig. 1b)

Fig. 4 The dependences of the effective average current density, $j_{av}*$, and the average current efficiency of hydrogen evolution, $\eta_{I,av}(H_2)$, on pause-to-pulse ratio. The current density amplitude 0.44 A/cm^2, pause duration 10 ms

Fig. 5 Cross section of the copper deposits obtained by the PC regimes with deposition pulses of **a** 4 ms, **b** 7 ms, **c** 10 ms, and **d** 20 ms. The current density amplitude 0.44 A/cm^2, pause duration 10 ms
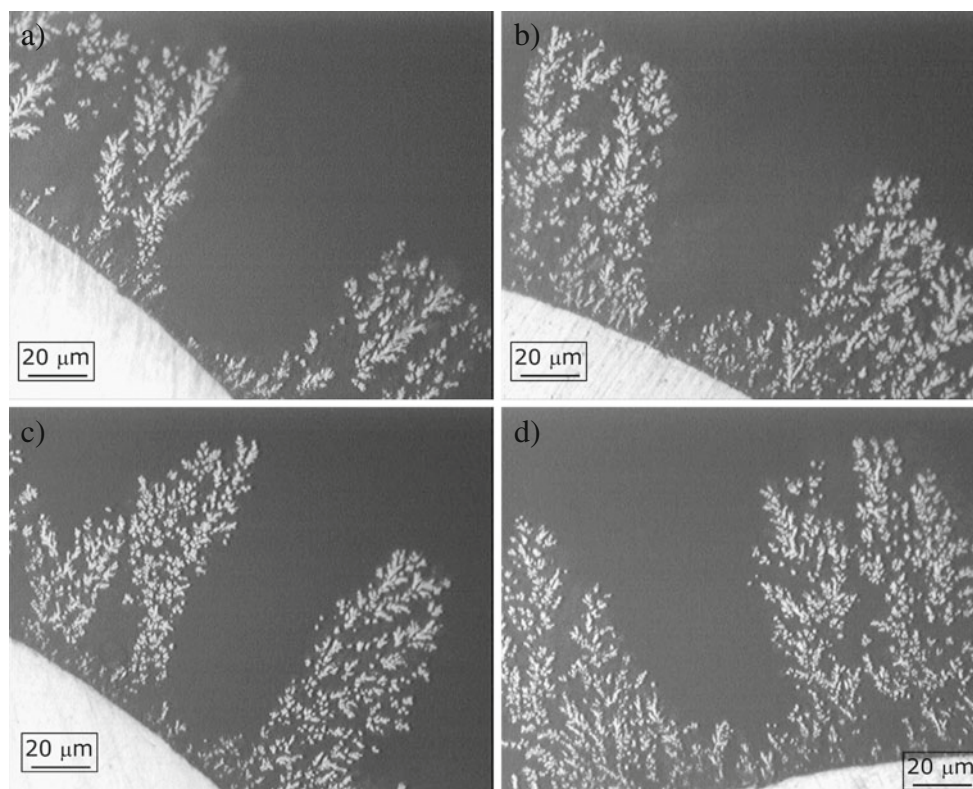
to agglomerates of grains formed around holes (Fig. 3d), clearly confirm the decrease of the degree of the diffusion control of electrodeposition process with the increase of the quantity of evolved hydrogen. It is very clear that the concept of "effective overpotential" is successfully applied for copper electrodeposition in the hydrogen co-deposition range by the PC regime. This concept applicable for the PC regimes is denoted as "effective overpotential amplitude" one.

The different degrees of diffusion control of electrodeposition process are attained by the choice of appropriate parameters of the square waves PC. For example, using the value j_A=0.20 A/cm^2, t_c=1 ms, and t_p=10 ms, as well as $\eta_{I,av}(H_2)$=5.5%, the effective average current density, j_{av}^*, calculated by the use of Eq. 12 was very close to the value of the limiting diffusion current density for this system (i.e., for 0.15 M CuSO$_4$ in 0.50 M H$_2$SO$_4$; $j_L \approx 16.0$ mA/cm^2 [3]). Hence, with these parameters of the PC regimes, electrodeposition process was controlled by the diffusion of ions to the electrode surface, what is confirmed by the formation of very branchy dendrites and small cauliflower-like agglomerates of copper grains (Fig. 1). Anyway, non-uniformity of the electrode surface clearly pointed out that the diffusion layer of the macroelectrode was not disturbed by evolved hydrogen during this electrodeposition process.

On the other hand, the increase of the effectiveness of solution stirring, the decrease of the cathode diffusion layer thickness, and the increase of the limiting diffusion current density occur with intensification of hydrogen evolution reaction leading to the formation of the honeycomb-like structures. The uniform distribution of morphological forms, i.e., holes and copper grains agglomerates, means the existence of the same hydrodynamic conditions over the whole electrode surface [5]. The size of grains in cauliflower-like agglomerates approached to nano-sized dimensions with the intensification of hydrogen evolution reaction, as shown in Fig. 6 for cauliflower-like ones
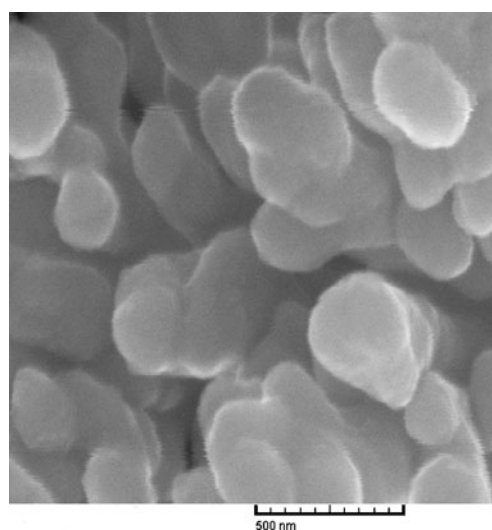

Fig. 6 Copper grains agglomerates obtained by the PC regime with a current density amplitude of 0.44 A/cm^2, a deposition pulse of 20 ms and a pause duration of 10 ms

obtained with t_c=20 ms. From Fig. 6, it can be clearly seen that the size of grains in these agglomerates is between 100 and 300 nm. Also, the porosity of the honeycomb-like structures was additionally increased by numerous nano-pores situated between copper grains, as observed from Fig. 6. The porous interior of these deposits is very important for electrocatalytic purposes because the pores facilitate the transport of electroactive species through the interior of the structures, what is very desirable for the evaluation of electrochemical reactions. For example, copper shows a high activity for nitrate ion reduction [30, 31], as well as for a reaction in which nitrate reduces to ammonia in high yield in aqueous acidic perchlorate and sulfate media [32].

Conclusions

Electrodeposition of copper in the hydrogen co-deposition range was examined by the square waves PC. The selected parameters of square waves PC, such as the current density amplitude, deposition pulse, and pause duration, strongly affected hydrogen evolution reaction and hence morphology of electrodeposited copper. The techniques of scanning electron and optical microscopes were used for the characterization of the formed deposits. In the dependence of selected parameters of the PC regime, the different degree of diffusion control of electrodeposition process can be attained. Effects attained by the application of the PC regime on morphology of electrodeposited copper in the hydrogen co-deposition range were equivalent to those obtained by electrodeposition in the potentiostatic regime at high overpotentials. The change of morphology of electrodeposited copper with the intensification of hydrogen evolution reaction was discussed by the application of the concept of "effective overpotential amplitude." This concept represents the expansion of existing concept of "effective overpotential" which was originally proposed to explain copper electrodeposition processes in the hydrogen co-deposition range by the potentiostatic regime of electrolysis. Analysis of morphologies of electrodeposited copper obtained by the selected parameters of square waves PC showed that this concept can be successfully applied for copper electrodeposition in the hydrogen co-deposition range by this pulse regime of electrolysis.

References

1. Nikolić ND, Popov KI (2010) Hydrogen co-deposition effects on the structure of electrodeposited copper. In: Djokić SS (ed) Modern aspects of electrochemistry, electrodeposition: theory and practice, vol 48. Springer, New York, pp 1–70
2. Shin HC, Dong J, Liu M (2003) Adv Mater 15:1610–1614
3. Nikolić ND, Popov KI, Pavlović LjJ, Pavlović MG (2006) J Electroanal Chem 588:88–98
4. Li Y, Jia W-Z, Song Y-Y, Xia X-H (2007) Chem Mater 19:5758–5764
5. Nikolić ND, Pavlović LjJ, Pavlović MG, Popov KI (2007) Electrochim Acta 52:8096–8104
6. Nikolić ND, Branković G, Pavlović MG, Popov KI (2008) J Electroanal Chem 621:13–21
7. Shin HC, Liu M (2005) Adv Funct Mater 15:582–586
8. Kim R, Han D, Nam D, Kim J, Kwon H (2010) J Electrochem Soc 157:D269–D273
9. Yin J, Jia J, Zhu L (2008) Int J Hydrogen Energy 33:7444–7447
10. Ortiz GF, Hanzu I, Knauth P, Lavela P, Tirado JL, Djenizian T (2009) Electrochim Acta 54:4262–4268
11. Ortiz GF, Hanzu I, Lavela P, Knauth P, Tirado JL, Djenizian T (2010) Chem Mater 22:1926–1932
12. Nikolić ND, Popov KI, Pavlović LjJ, Pavlović MG (2007) J Solid State Electrochem 11:667–675
13. Nikolić ND, Popov KI, Pavlović LjJ, Pavlović MG (2007) Sensors 7:1–15
14. Marozzi CA, Chialvo AC (2000) Electrochim Acta 45:2111–2120
15. Cherevko S, Xing X, Chung C-H (2010) Electrochem Commun 12:467–470
16. Cherevko S, Chung C-H (2010) Electrochim Acta 55:6383–6390
17. Nikolić ND, Maksimović VM, Pavlović MG, Popov KI (2009) J Serb Chem Soc 74:689–696
18. Nikolić ND, Branković G, Pavlović MG, Popov KI (2009) Electrochem Commun 11:421–424
19. Nikolić ND, Branković G, Maksimović VM, Pavlović MG, Popov KI (2009) J Electroanal Chem 635:111–119
20. Nikolić ND, Branković G, Maksimović VM, Pavlović MG, Popov KI (2010) J Solid State Electrochem 14:331–338
21. Nikolić ND, Branković G, Popov KI (2011) Mater Chem Phys 125:587–594
22. Shin HC, Liu M (2004) Chem Mater 16:5460–5464
23. Kim J-H, Kim R-H, H-Sang K (2008) Electrochem Commun 10:1148–1151
24. Popov KI, Maksimović MD (1989) Theory of the effect of electrodeposition at a periodically changing rate on the morphology of metal deposits. In: Conway BE, Bockris JO'M, White RE (eds) Modern aspects of electrochemistry, vol 19. Plenum, New York, pp 193–250
25. Chandrasekar MS, Pushpavanam M (2008) Electrochim Acta 53:3313–3322
26. Nikolić ND, Branković G (2010) Electrochem Commun 12:740–744
27. Popov KI, Pavlović MG (1993) Electrodeposition of metal powders with controlled grain size and morphology. In: White RE, Bockris JO'M, Conway BE (eds) Modern aspects of electrochemistry, vol 24. Plenum, New York
28. Popov KI, Djokić SS, Grgur BN (2002) Fundamental aspects of electrometallurgy. Kluwer Academic, New York
29. Pavlović MG, Nikolić ND, Popov KI (2003) J Serb Chem Soc 68:649–656
30. Dima GE, De Vooys ACA, Koper MTM (2003) J Electroanal Chem 554–555:15–23
31. Ko W-Y, Chen W-H, Cheng C-Y, Lin K-J (2009) Sens Actuators B 137:437–441
32. Pletcher D, Poorbedi Z (1979) Electrochim Acta 24:1253–1256